

Clusters, lensing and CFHT reprocessing

R. Ansari - French LSST meeting
December 2015

- ◆ Clusters as cosmological probes
- ◆ Clusters: characteristics and properties
- ◆ Basics of lensing
- ◆ Weighting the Giants
- ◆ Clusters and CFHT reprocessing

Clusters as cosmological probes

$$\frac{dN}{dzdM_O} = \frac{dV}{dz}(z, \Theta_C) \int d \ln M P(M_O|M, z, \Theta_N) \Pi(M, z, \Theta_N) \frac{dn}{d \ln M}(M, z, \Theta_C) + \left. \frac{dN}{dzdM_O} \right|_{false}$$

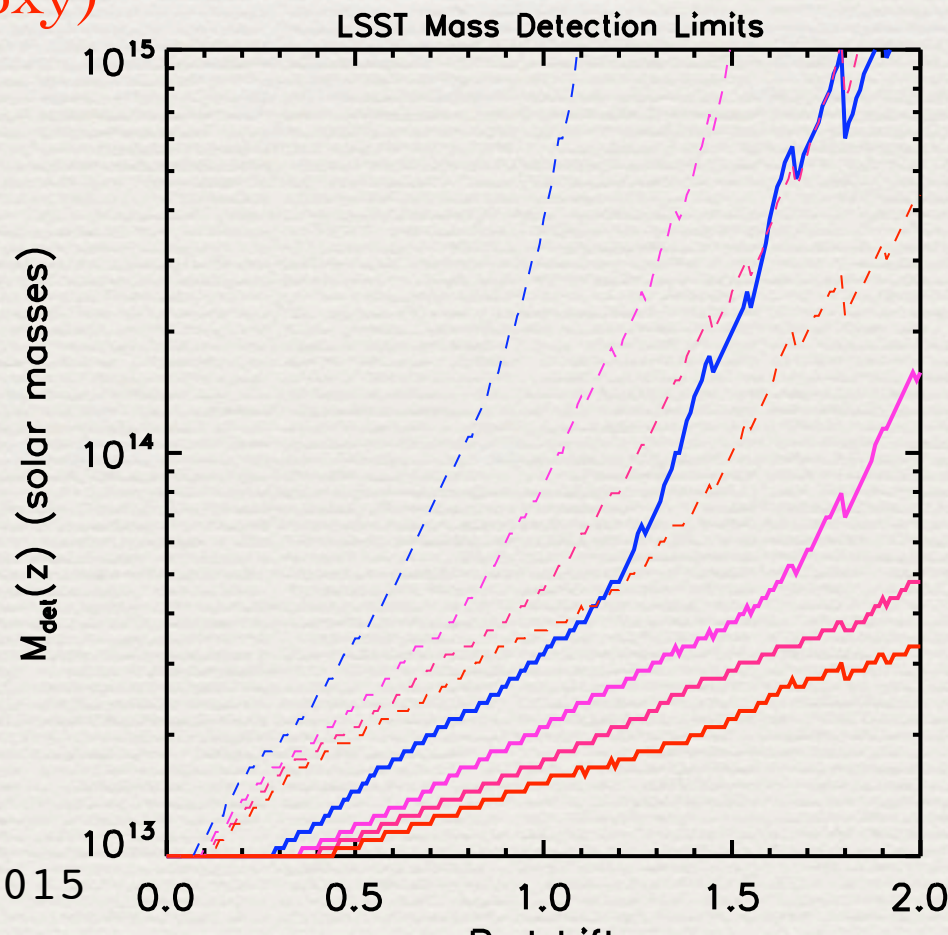
Cluster number count, as a function of redshift and Observed mass (or mass proxy)

Volume element, depends on cosmological parameters (/ Geometry) Θ_C

Cluster (astro)physics

$$\frac{dn}{d \ln M} = \frac{\bar{\rho}}{M} F(M, z, \Theta_C)$$

Cluster mass function, depends on cosmology and mean matter density

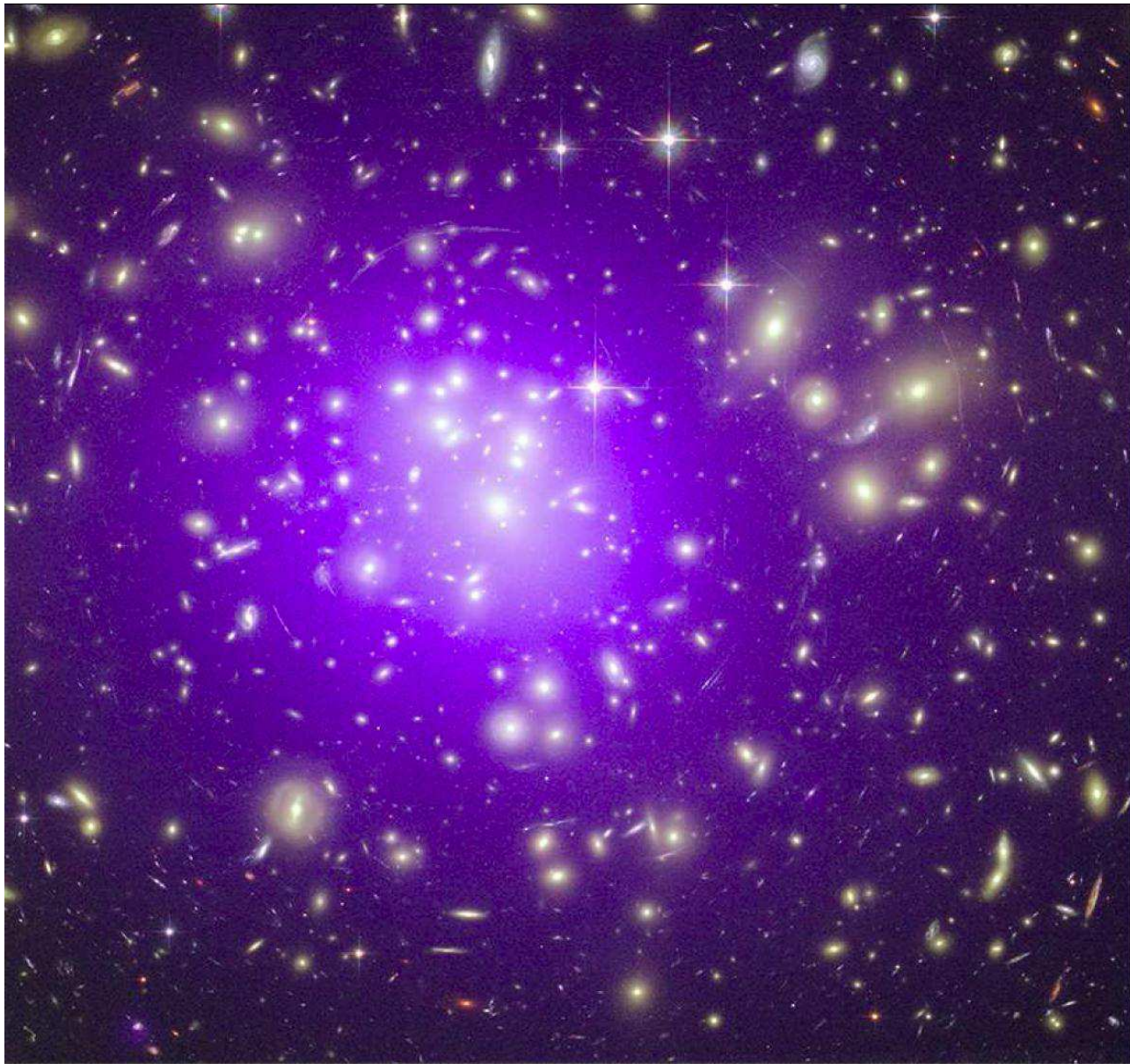


Cluster mass detection limit in r,i,z,y bands (blue-red) - dashed: single visit, solid: 10 years survey

Cluster properties

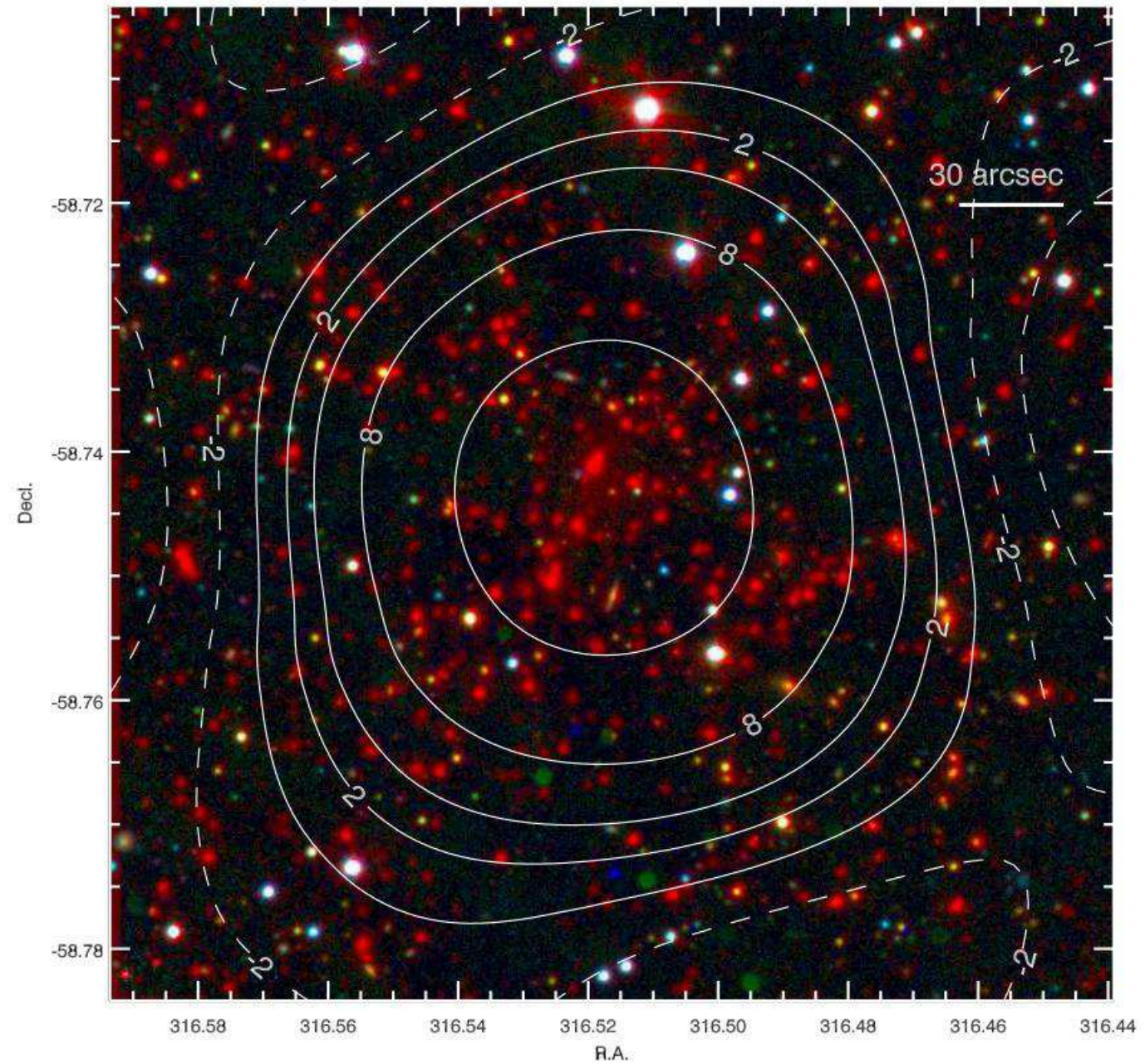
- ♦ Most massive and largest gravitationally bound systems in the universe
- ♦ Typical sizes: 2-10 Mpc, typical masses: 10^{13} - $10^{15} M_{\text{sol}}$ - 100-1000 galaxies - mean over densities : $\delta\rho/\rho \sim 100$ -1000
- ♦ Galaxies, hot gas (x-ray emitting), dark matter
- ♦ Red galaxies (elliptical) / BCG , with old stars and little gas in the central region - spiral galaxies in the outer regions
- ♦ Observed as group of galaxies in optical surveys, extended x-ray emitting sources (hot gas) or through the SZ effect in microwave (CMB)

Andrey V. Kravtsov¹ and Stefano Borgani², Annual Review of Astronomy and Astrophysics, (2012)



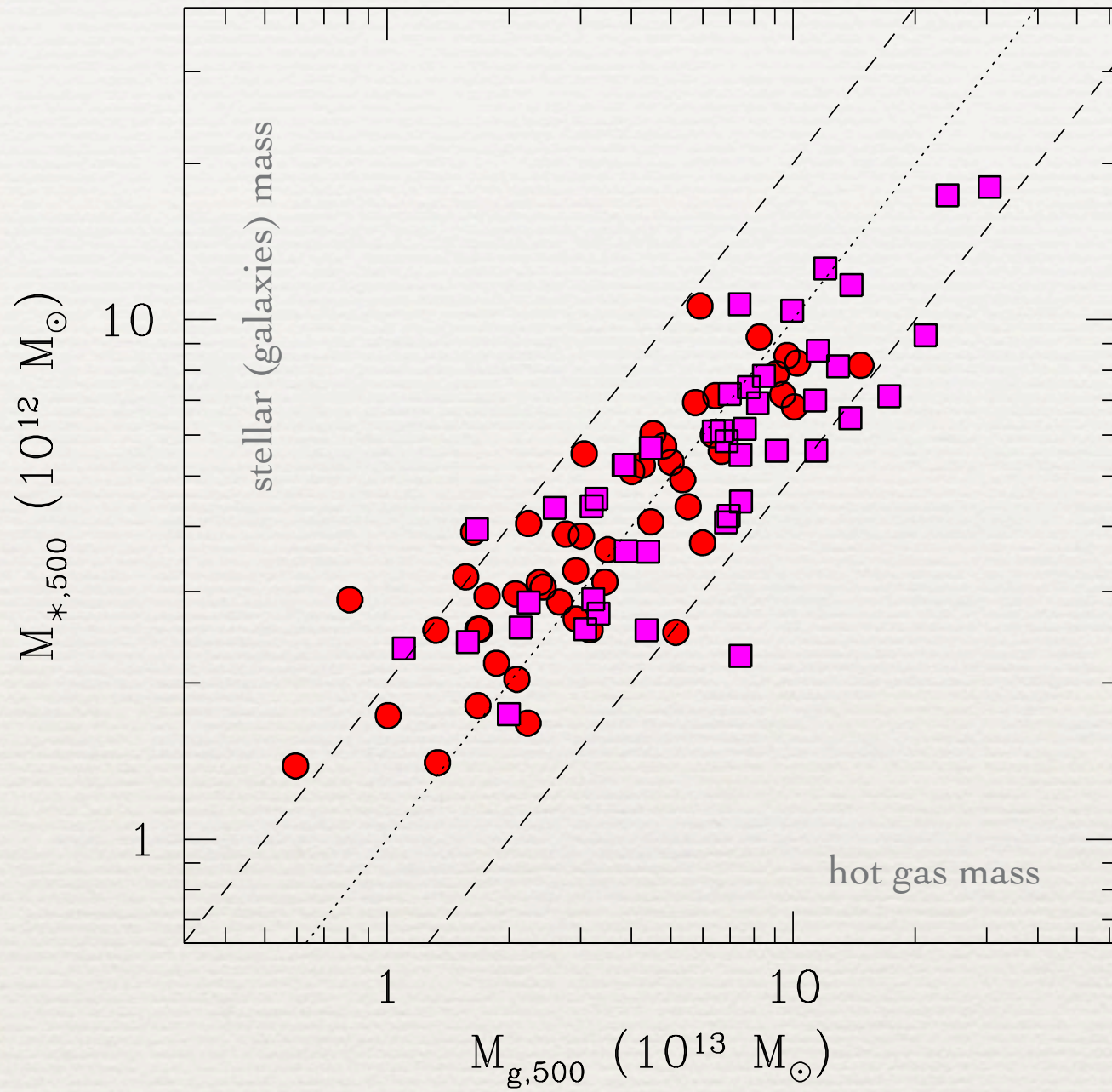
1.8 arcmin = 556 kpc

Abell 1689 , $z=0.18$
 HST (optical) +
 Chandra (xray image)
 giant arcs



4.8 arcmin = 2.4 Mpc

SPT-CLJ2106-5844 ,
 $z=1.133$ Optical / IR
 (Spitzer image) + SZ
 contours (SPT)



Mstars ~ 0.1 Mgas

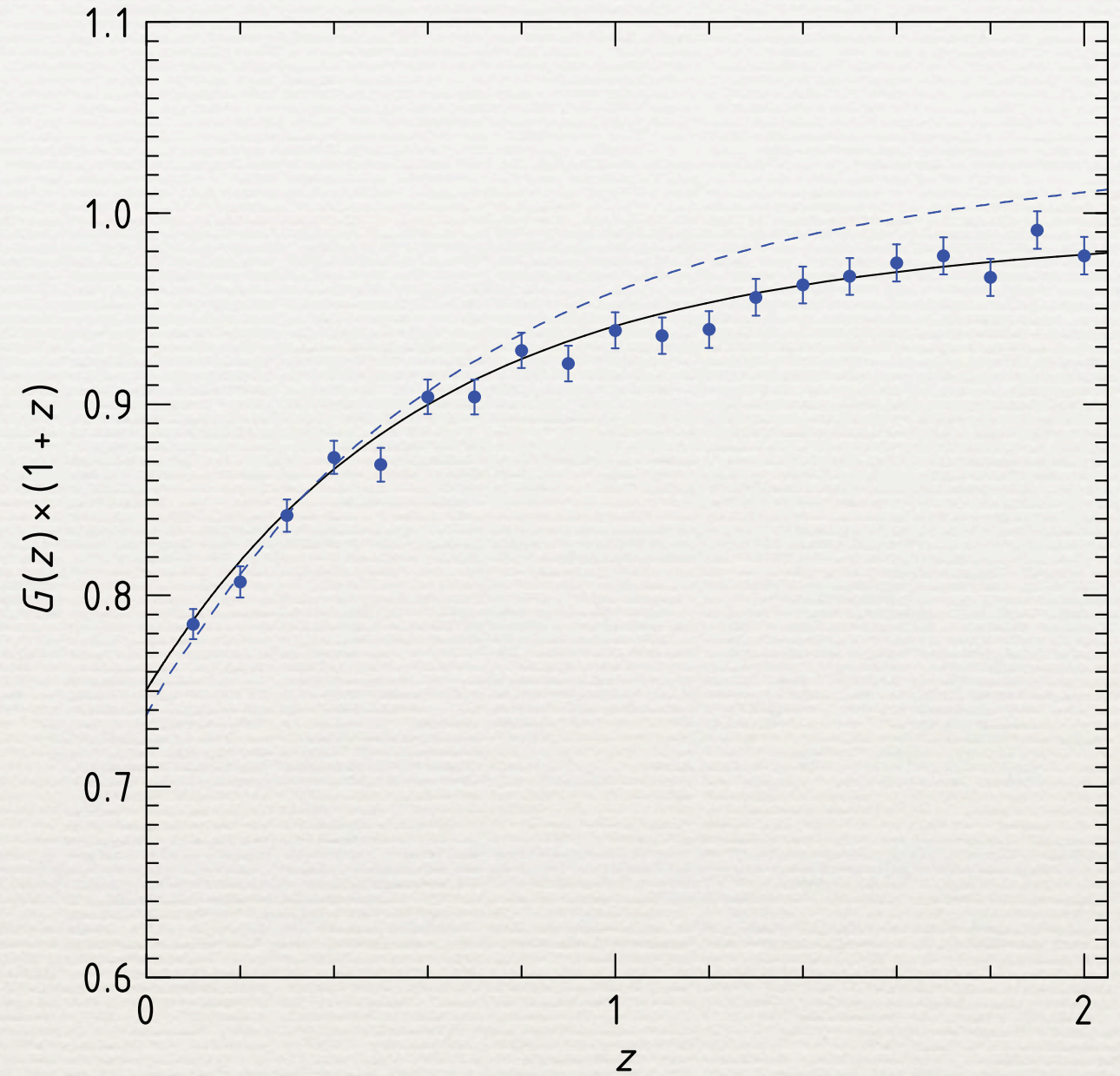


Fig. 17. The potential of future cluster surveys to constrain deviations from General Relativity (from Vikhlinin et al. 2009d). The linear growth factor of density perturbations, $G(z) = D(z)$ (not normalized to unity at $z = 0$), recovered from 2000 clusters, distributed in 20 redshift bins, each containing 100 massive clusters, identified in a high-sensitivity X-ray cluster survey. The solid black line indicates the evolution of the linear growth factor for a Λ CDM model, whereas the dashed blue curve is the prediction of a modified gravity model (the brane world model by Dvali, Gabadadze & Porrati 2000), having the same expansion history of the Λ CDM model.

Andrey V. Kravtsov¹ and Stefano Borgani², Annual Review of Astronomy and Astrophysics, (2012)

Lensing (I)

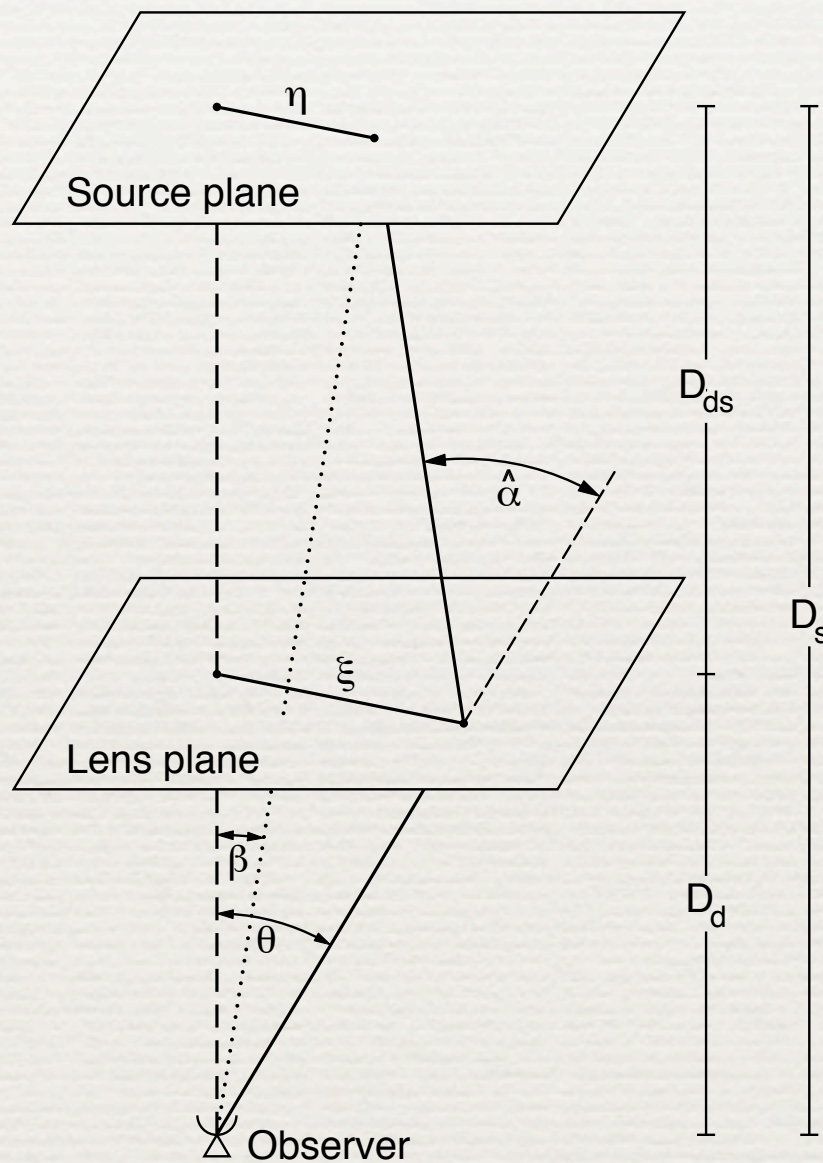


Fig. 11. Sketch of a typical gravitational lens system.

1. Lensing by a point mass M , deflection angle α , for an impact parameter ξ in the deflector plane. R_S is the schwarzschild radius. The deflection angle is small for $\xi \gg R_S$.

$$R_S = 2 \frac{GM}{c^2}$$

$$\hat{\alpha} = 4 \frac{GM}{c^2 \xi} = 2 \frac{R_S}{\xi}$$

2. Introducing the distances to the source D_s to the deflector or lens D_d and deflector-source distance D_{ds} , we can then compute the Einstein ring radius R_E . Notice that angular diameter distances should be used in FRW cosmology.

$$D = \frac{D_d D_{ds}}{D_s}$$

$$R_E = 4 \frac{GM D}{c^2}$$

Lensing (II)

1. For a lens characterized by a surface mass distribution, or projected mass distribution $\Sigma(\xi)$, the deflection angle can be written as :

$$\hat{\alpha}(\vec{\xi}) = \frac{4G}{c^2} \int d^2\xi' \Sigma(\xi') \frac{\vec{\xi} - \vec{x}i'}{|\vec{\xi} - \vec{\xi}'|^2}$$

2. Introducing the angular coordinates $\vec{\beta}$ in the source plane and $\vec{\theta}$ in the deflector plane ($\vec{\eta} = D_s\vec{\beta}$, $\vec{\xi} = D_d\vec{\theta}$), we can define the lens equation, relating the angular position in the source plane and the deflector plane, to the reduced angular deflection:

$$\begin{aligned} \vec{\beta} &= \vec{\theta} - \vec{\alpha}(\vec{\theta}) \\ \vec{\alpha}(\vec{\theta}) &= \frac{D_{ds}}{D_s} \hat{\alpha}(D_d\vec{\theta}) \end{aligned}$$

3. Introducing the critical mass density which depends on the distances, and the mass density ratio κ :

$$\begin{aligned} \Sigma_{cr} &= \frac{c^2}{4\pi G} \frac{D_s}{D_d D_{ds}} \\ \kappa(\vec{\theta}) &= \frac{\Sigma(D_d\vec{\theta})}{\Sigma_{cr}} \end{aligned}$$

4. the deflection angle $\vec{\alpha}(\theta)$ can be written as the gradient of the deflection potential :

$$\begin{aligned} \vec{\alpha}(\vec{\theta}) &= \frac{1}{\pi} \int_{\mathbb{R}^2} d^2\theta' \kappa(\vec{\theta}') \frac{\vec{\theta} - \vec{\theta}'}{|\vec{\theta} - \vec{\theta}'|^2} \\ \psi(\vec{\theta}) &= \int_{\mathbb{R}^2} d^2\theta' \kappa(\vec{\theta}') \ln |\vec{\theta} - \vec{\theta}'| \\ \nabla^2 \psi(\vec{\theta}) &= 2\kappa(\vec{\theta}) \quad \vec{\alpha}(\vec{\theta}) = \vec{\nabla} \psi(\vec{\theta}) \end{aligned}$$

Lensing (III)

1. The observed surface brightness distribution in the lens plane $I(\vec{\theta})$ can be written as a function of the source plane surface brightness distribution $I^s(\vec{\beta})$

$$I(\vec{\theta}) = I^s(\vec{\beta}(\vec{\theta})) \quad \vec{\beta}(\vec{\theta}) = \vec{\theta} - \vec{\alpha}(\vec{\theta})$$

2. Linearizing the equation, we can define the lens mapping matrix \mathcal{A} :

$$I(\vec{\theta}) = I^s \left[\vec{\beta}_0 + \mathcal{A}(\vec{\theta}_0) (\vec{\theta} - \vec{\theta}_0) \right]$$

$$\mathcal{A}(\vec{\theta}) = \frac{\partial \vec{\beta}}{\partial \vec{\theta}} = \left(\delta_{ij} - \frac{\partial^2 \psi(\vec{\theta})}{\partial \theta_i \partial \theta_j} \right)$$

$$\mathcal{A} = \begin{pmatrix} 1 - \kappa - \gamma_1 & -\gamma_2 \\ -\gamma_2 & 1 - \kappa + \gamma_1 \end{pmatrix}$$

3. κ corresponds to the convergence and $\gamma = \gamma_1 + i\gamma_2 = |\gamma|e^{2i\varphi}$ is the shear. The eigenvalues of \mathcal{A} are $1 - \kappa \pm |\gamma|$.

$$\gamma_1 = \frac{1}{2}(\psi_{11} - \psi_{22}) \quad \gamma_2 = \psi_{12} = \frac{\partial^2 \psi}{\partial \theta_1 \partial \theta_2}$$

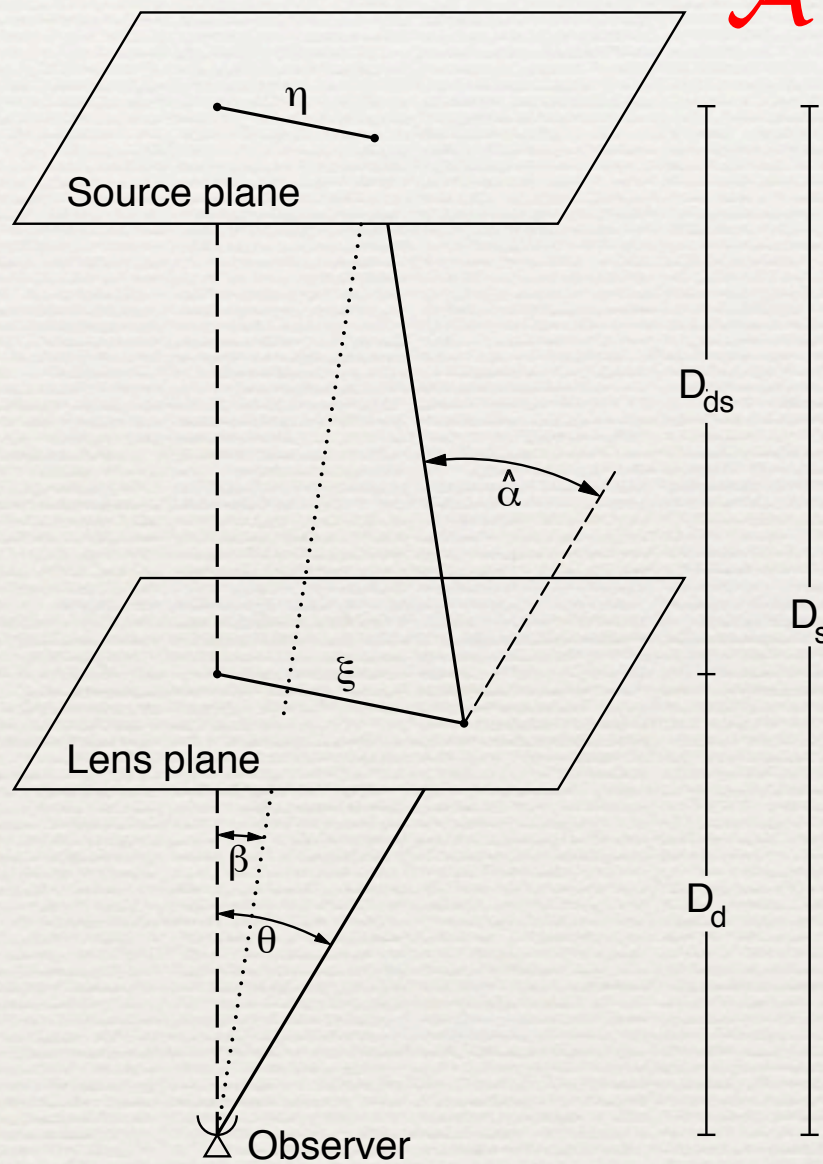
4. The surface brightness is conserved. The image of a circular source is an ellipse with the ratio of the two axis (the ellipticity ϵ) given by the ratio of the two eigenvalues. the magnification μ corresponds to ratio of solid angles.

$$\mu = \frac{1}{\det \mathcal{A}} = \frac{1}{(1 - \kappa)^2 - |\gamma|^2}$$

$$\epsilon = \frac{1 - \kappa - |\gamma|}{1 - \kappa + |\gamma|}$$

Lensing (summary)

(local) lensing mapping matrix



$$\mathcal{A}(\vec{\theta}) =$$

$$\begin{pmatrix} 1 - \kappa - \gamma_1 & -\gamma_2 \\ -\gamma_2 & 1 - \kappa + \gamma_1 \end{pmatrix}$$

shear \rightarrow ellipticities

$$\gamma = \gamma_1 + i\gamma_2$$

$$\gamma_1 = \frac{1}{2} \left(\frac{\partial^2 \psi}{\partial \theta_1 \partial \theta_1} - \frac{\partial^2 \psi}{\partial \theta_2 \partial \theta_2} \right)$$

$$\gamma_2 = \frac{\partial^2 \psi}{\partial \theta_1 \partial \theta_2}$$

lensing potential

$$\nabla^2 \psi(\vec{\theta}) = 2\kappa(\vec{\theta})$$

2D (projected) mass density

$$\kappa(\vec{\theta}) = \frac{\Sigma(D_d \vec{\theta})}{\Sigma_{cr}}$$

critical density,
includes distances

Fig. 11. Sketch of a typical gravitational lens system.

M. Bartelmann & P. Schneider, *Weak Gravitational Lensing*
Phys. Reports (2001) arXiv:9912508

R. Ansari 12/2015

Monday 7 December 15

Weighting the Giants

Weighing the Giants I. Weak-lensing masses for 51 massive galaxy clusters: project overview, data analysis methods and cluster images

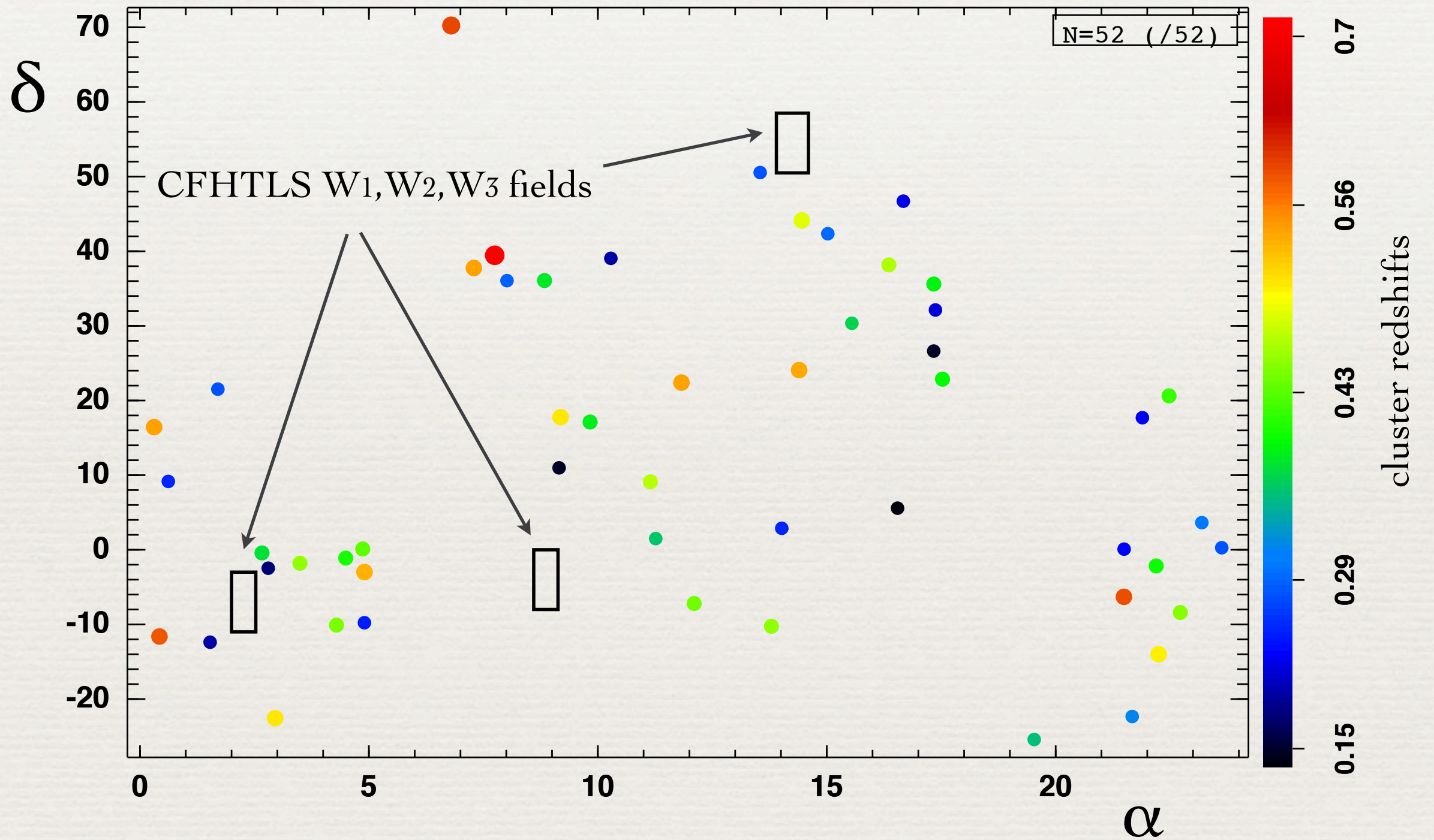
Anja von der Linden^{1,2,3} [★], Mark T. Allen^{1,2}, Douglas E. Applegate^{1,2,4,5}, Patrick L. Kelly^{1,2,4,6}, Steven W. Allen^{1,2,4}, Harald Ebeling⁷, Patricia R. Burchat^{1,2}, David L. Burke^{1,4}, David Donovan⁷, R. Glenn Morris^{1,4}, Roger Blandford^{1,2,4}, Thomas Erben⁵, Adam Mantz^{8,9}

ABSTRACT

This is the first in a series of papers in which we measure accurate weak-lensing masses for 51 of the most X-ray luminous galaxy clusters known at redshifts $0.15 \lesssim z_{\text{Cl}} \lesssim 0.7$, in order to calibrate X-ray and other mass proxies for cosmological cluster experiments. The primary aim is to improve the absolute mass calibration of cluster observables, currently the dominant systematic uncertainty for cluster count experiments. Key elements of this work are the rigorous quantification of systematic uncertainties, high quality data reduction and photometric calibration, and the “blind” nature of the analysis to avoid confirmation bias. Our target clusters are drawn from X-ray catalogs based on the ROSAT All-Sky Survey, and provide a versatile calibration sample for many aspects of cluster cosmology. We have acquired wide-field, high-quality imaging using the Subaru and CFHT telescopes for all 51 clusters, in at least three bands per cluster. For a subset of 27 clusters, we have data in at least five bands, allowing accurate photometric redshift estimates of lensed galaxies. In this paper, we describe the cluster sample and observations, and detail the processing of the SuprimeCam data to yield high-quality images suitable for robust weak-lensing shape measurements and precision photometry. For each cluster, we present wide-field three-color optical images and maps of the weak-lensing mass distribution, the optical light distribution, and the X-ray emission. These provide insights into the large-scale structure in which the clusters are embedded. We measure the offsets between X-ray flux centroids and the Brightest Cluster Galaxies in the clusters, finding these to be small in general, with a median of 20 kpc. For offsets $\lesssim 100$ kpc, weak-lensing mass measurements centered on the Brightest Cluster Galaxies agree well with values determined relative to the X-ray centroids; miscentering is therefore not a significant source of systematic uncertainty for our weak-lensing mass measurements. In accompanying papers we discuss the key aspects of our photometric calibration and photometric redshift measurements (Kelly et al.), and measure cluster masses using two methods, including a novel Bayesian weak-lensing approach that makes full use of the photometric redshift probability distributions for individual background galaxies (Applegate et al.). In subsequent papers, we will incorporate these weak-lensing mass measurements into a self-consistent framework to simultaneously determine cluster scaling relations and cosmological parameters.

[arXiv1208.0597](https://arxiv.org/abs/1208.0597)

51 x-ray selected (ROSAT) clusters



Weighing The Giants - III. Methods and Measurements of Accurate Galaxy Cluster Weak-Lensing Masses

Douglas E. Applegate^{1,2,3,4} [★], Anja von der Linden^{1,2,5}, Patrick L. Kelly^{1,2,3}, Mark T. Allen^{1,2}, Steven W. Allen^{1,2,3}, Patricia R. Burchat^{1,2}, David L. Burke^{1,3}, Harald Ebeling⁶, Adam Mantz^{7,8}, R. Glenn Morris^{1,3}

ABSTRACT

We report weak-lensing masses for 51 of the most X-ray luminous galaxy clusters known. This cluster sample, introduced earlier in this series of papers, spans redshifts $0.15 \lesssim z_{cl} \lesssim 0.7$, and is well suited to calibrate mass proxies for current cluster cosmology experiments. Cluster masses are measured with a standard ‘color-cut’ lensing method from three-filter photometry of each field. Additionally, for 27 cluster fields with at least five-filter photometry, we measure high-accuracy masses using a new method that exploits all information available in the photometric redshift posterior probability distributions of individual galaxies. Using simulations based on the COSMOS-30 catalog, we demonstrate control of systematic biases in the mean mass of the sample with this method, from photometric redshift biases and associated uncertainties, to better than 3%. In contrast, we show that the use of single-point estimators in place of the full photometric redshift posterior distributions can lead to significant redshift-dependent biases on cluster masses. The performance of our new photometric redshift-based method allows us to calibrate ‘color-cut’ masses for all 51 clusters in the present sample to a total systematic uncertainty of $\approx 7\%$ on the mean mass, a level sufficient to significantly improve current cosmology constraints from galaxy clusters. Our results bode well for future cosmological studies of clusters, potentially reducing the need for exhaustive spectroscopic calibration surveys as compared to other techniques, when deep, multi-filter optical and near-IR imaging surveys are coupled with robust photometric redshift methods.

[arXiv1208.0605](https://arxiv.org/abs/1208.0605)

shear, convergence
for source at infinity

reduced shear

The ellipticity of a galaxy, corrected for PSF effects, provides a noisy estimate of the reduced shear at the galaxy position. Assuming a single lens plane, the theoretical expectation for the reduced shear $g(\vec{\theta})$ is given by

$$g(\vec{\theta}) = \frac{\beta_s(z_b)\gamma_\infty(\vec{\theta})}{1 - \beta_s(z_b)\kappa_\infty(\vec{\theta})}, \quad (1)$$

where the shear $\gamma_\infty(\vec{\theta})$ and convergence $\kappa_\infty(\vec{\theta})$ are set by the mass distribution of the lens, evaluated at the source position $\vec{\theta}$, assuming a lensed source at infinite redshift. For an axisymmetric lens, Eq. 1 reduces to a scalar equation, as the only shear will be tangential to the lens. The dependence of the distortion on the background-galaxy redshift is set by $\beta_s(z_b)$:

$$\beta_s = \frac{D_{LS}}{D_S} \frac{D_\infty}{D_{L,\infty}}.$$

correction term for
source distance

arXiv1208.0605

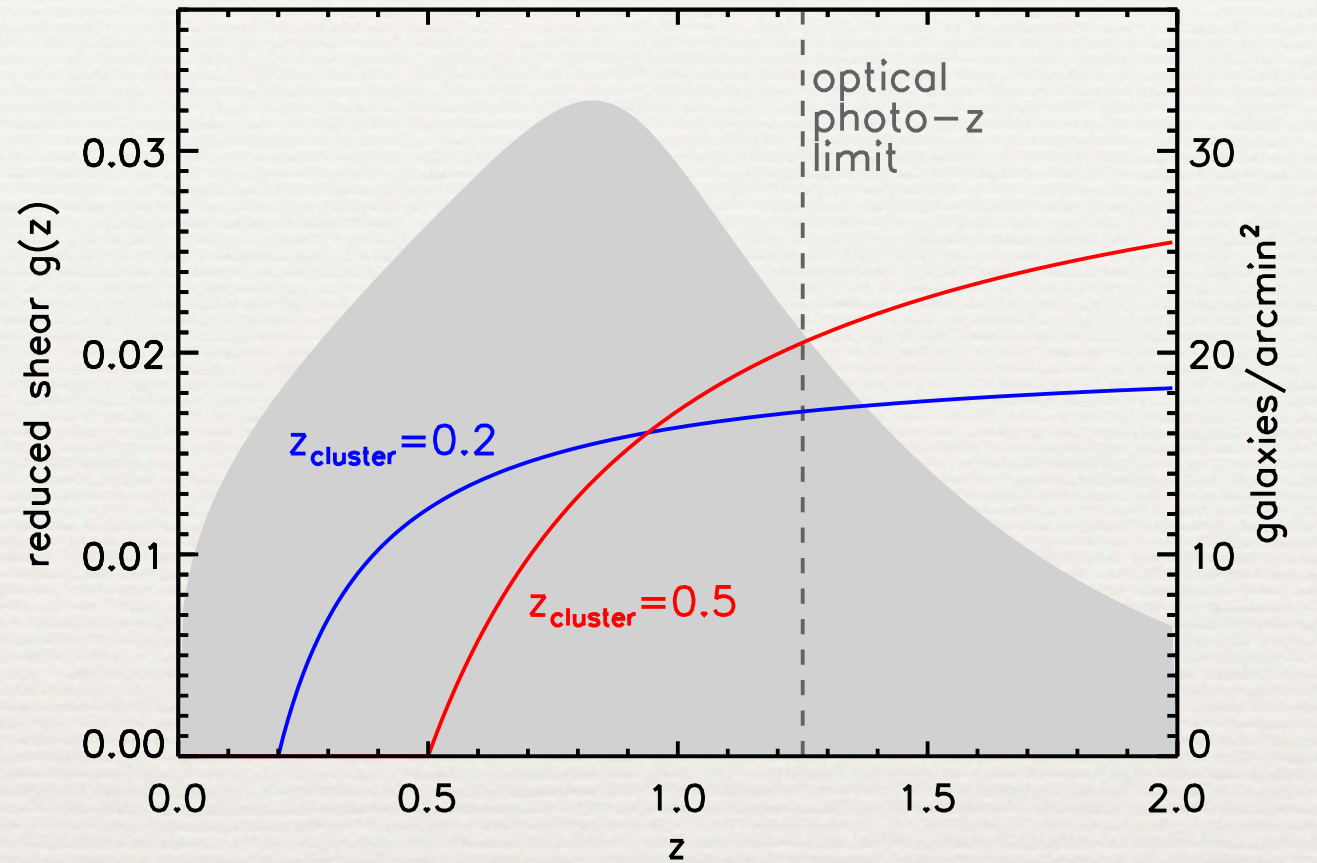


Figure 1. The reduced shear g , as a function of source galaxy redshift z , for cluster lenses at redshifts $z_{\text{cluster}} = 0.2$ and 0.5 . The function β_s , a ratio of angular diameter distances, controls the shape of the curve (see Eq. 2). β_s is zero for sources at redshifts less than z_{cluster} and rises steeply above z_{cluster} , eventually flattening off at high redshift. The shape of the function is cosmology dependent. A typical galaxy redshift distribution for a typical ground-based $i^+ < 25$ mag survey is shown in light gray, peaking at $z \approx 0.8$.

CFHT reprocessing

- ♦ Testing and validating the stack
- ♦ galaxy photometry and shape determination
- ♦ accurate photometry / colors for photoZ
- ♦ PSF quality after stacking in order to extract galaxy shape parameters
- ♦ Currently: Abell 2261 and Abell 1835 (??)

<https://github.com/DarkEnergyScienceCollaboration/ReprocessingTaskForce/wiki/CFHT-Clusters>

Galaxy Cluster Abell 2261
Hubble Space Telescope

ACS/WFC F435W F475W
ACS/WFC F8606W F625W F775W
ACS/WFC F814W F850LP
WFC3/IR F105W F110W F125W F140W F160W

500,000 light-years
153 kiloparsecs 48''



Abell 2261 $z \sim 0.22$

<http://hubblesite.org/newscenter/archive/releases/2012/24/fastfacts/>

R. Ansari 12/2015

About the Object

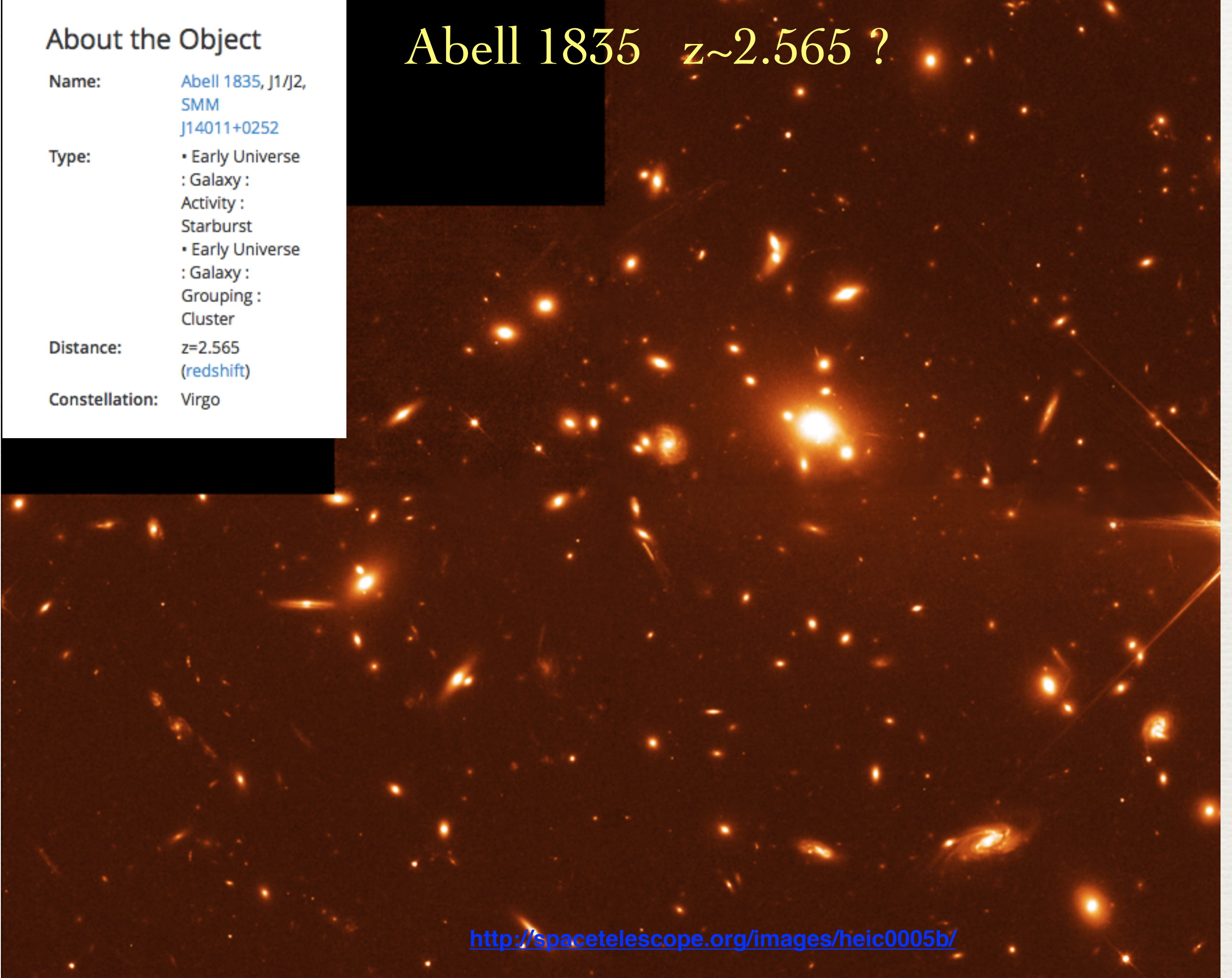
Name: Abell 1835, J1/J2,
SMM
J14011+0252

Type: • Early Universe
: Galaxy :
Activity :
Starburst
• Early Universe
: Galaxy :
Grouping :
Cluster

Distance: $z=2.565$
(redshift)

Constellation: Virgo

Abell 1835 $z \sim 2.565$?



<http://spacetelescope.org/images/heic0005b/>